Drug Design, Development and Therapy

Dovepress
open access to scientific and medical research

Open Access Full Text Article

ORIGINAL RESEARCH

Pristimerin Inhibits Osteoclast Differentiation and Bone Resorption in vitro and Prevents Ovariectomy-Induced Bone Loss in vivo

This article was published in the following Dove Press journal:
Drug Design, Development and Therapy

Drug Design, Development and Therapy downloaded from https://www.dovepress.com/
For personal use only.

Peng Sun[1,2]
Qichang Yang[1]
Yanben Wang[2]
Jiaxuan Peng[3]
Kangxian Zhao[1]
Yewei Jia[2]
Tan Zhang[2]
Xuanyuan Lu[2]
Weiqi Han[2]
Yu Qian[1,2]

[1]The Second Affiliated Hospital and Yuying Children's Hospital of Wenzhou Medical University, Wenzhou, Zhejiang 325000, People's Republic of China; [2]Department of Orthopedics, Shaoxing People's Hospital (Shaoxing Hospital, Zhejiang University School of Medicine), Shaoxing, Zhejiang 312000, People's Republic of China; [3]Guangxi Key Laboratory of Regenerative Medicine, Guangxi Medical University, Nanning, Guangxi 530021, People's Republic of China

Introduction: Osteoporosis is a metabolic bone disease characterized by reduced bone quantity and microstructure, typically owing to increased osteoclastogenesis and/or enhanced osteoclastic bone resorption, resulting in uncontrolled bone loss, which primarily affects postmenopausal women. In consideration of the severe side effects of current drugs for osteoporosis, new safe and effective medications are necessary. Pristimerin (Pri), a quinone methide triterpene extracted from Celastraceae and Hippocrateaceae members, exhibits potent antineoplastic and anti-inflammatory effects. However, its effect on osteoclasts remains unknown.

Materials and Methods: We evaluated the anti-osteoclastogenic and anti-resorptive effect of Pri on bone marrow-derived osteoclasts and its underlying mechanism in vitro. In addition, the protective effect of Pri on ovariectomy model was also explored in vivo.

Results: In vitro, Pri inhibited osteoclast differentiation and mature osteoclastic bone resorption in a time- and dose-dependent manner. Further, Pri suppressed the expression of osteoclast-related genes and the activation of key proteins. Pri also inhibited the early activation of ERK, JNK MAPK, and AKT signaling pathways in bone marrow-derived macrophages (BMMs), ultimately inhibiting the induction and activation of the crucial osteoclast transcriptional factor nuclear factor of activated T-cell cytoplasmic 1 (NFATc1). In vivo, consistent with our in vitro data, Pri clearly prevented ovariectomy-induced bone loss.

Conclusion: Our data showed that Pri inhibits the differentiation and activation of osteoclasts in vitro and in vivo, and could be a promising candidate for treating osteoporosis.

Keywords: osteoclast, osteoporosis, ERK, JNK, AKT, Pri

Introduction

Bone homeostasis relies on the balance between the resorption of bones by osteoclasts and formation of bones by the osteoblasts.[1] Osteoclasts are the cells responsible for bone resorption, a process critical to maintaining healthy bones.[2] Dysregulation of osteoclastic bone resorption could cause osteoporosis and malignant osteolytic bone disease.[3] Osteoporosis is a common systemic skeletal disorder that primarily affects the aged especially postmenopausal women and results in fragility fracture and increased mortality.[4,5] Thus, there is an urgent need for the development of new treatments for osteoporosis, considering the multiple side effects of the drugs currently in use.[6,7]

Monocyte/macrophage lineage cells differentiate into preosteoclasts under the stimulation of macrophage colony-stimulating factor (M-CSF) and receptor activation of NF-κB ligand (RANKL). Subsequently, preosteoclasts fuse and differentiate

Correspondence: Yu Qian
The Second Affiliated Hospital and Yuying Children's Hospital of Wenzhou Medical University, No. 109, XueYuan Road, Wenzhou, Zhejiang 325000, People's Republic of China
Email doctor120@hotmail.com

submit your manuscript | www.dovepress.com
DovePress
http://doi.org/10.2147/DDDT.S275128

© 2020 Sun et al. This work is published and licensed by Dove Medical Press Limited. The full terms of this license are available at https://www.dovepress.com/terms.php and incorporate the Creative Commons Attribution – Non Commercial (unported, v3.0) License (http://creativecommons.org/licenses/by-nc/3.0/). By accessing the work you hereby accept the Terms. Non-commercial uses of the work are permitted without any further permission from Dove Medical Press Limited, provided the work is properly attributed. For permission for commercial use of this work, please see paragraphs 4.2 and 5 of our Terms (https://www.dovepress.com/terms.php).

into functional mature multinucleated osteoclasts.[8] The cytokine M-CSF, a prerequisite for the induction of osteoclast, promotes the proliferation and survival of preosteoclasts and induces the binding of RANKL with its receptor RANK on the cell membrane.[9] RANKL activates a variety of downstream signaling pathways such as NF-κB, MAPKs, and PI3K/AKT to induce transcription and expression of osteoclastic key transcriptional factors such as tartrate-resistant acid phosphatase (TRAP), CTSK, c-Fos, and NFATc1, eventually inducing the formation of mature osteoclasts with the main function of bone resorption.[10,11]

Pristimerin (Pri) is a naturally occurring quinone methide triterpene extracted from Celastraceae and Hippocrateaceae members.[12] It has been shown to exert anti-cancer, anti-inflammatory, and antiperoxidative effects.[13–15] It is also reported that Pri enhances recombinant adeno-associated virus vector-mediated transgene expression in human cell lines in vitro and murine hepatocytes in vivo.[16] Furthermore, another study reported that Pri could suppress the NF-κB and MAPK signaling pathway.[17] Therefore, we explored potential Pri inhibitory effects on RANKL-induced osteoclastogenesis and bone resorption. In our study, the effect of Pri on RANKL-induced osteoclast formation and its potential mechanism in vitro, as well as its osteoprotective property in vivo were investigated.

Materials and Methods

Media and Reagents

Pristimerin was purchased from MedChemExpress (New Jersey, USA, purity >99%), dissolved in dimethyl sulfoxide (DMSO) at stock concentration of 10 mM and stored −20°C. Alpha-modified minimal essential medium (α-MEM) was from Hyclone (GE Healthcare, Chicago, IL, USA). Fetal bovine serum (FBS), penicillin, and streptomycin were obtained from Gibco (Thermo Fisher Scientific, Waltham, MA, USA). M-CSF and RANKL were procured from R&D Systems (Minneapolis, MN, USA). The F-actin cytoskeleton staining kit was purchased from Millipore (Darmstadt, Germany). Antibodies against NF-κB, AKT, MAPK, c-Fos, and c-Jun were purchased from Cell Signaling Technology (dilution 1:1000; Danvers, MA, USA). Specific primary antibody against NFATc1 was from Abcam (dilution 1:1000; Cambridge, UK).

Cell Culture

Mouse BMMs were isolated from bone marrow of 6-week-old C57BL/6 mice by flushing the tibias and femurs with culture media. BMMs were maintained in complete α-MEM with 1% P/S, 10% FBS and 25 ng/mL M-CSF for about 3 days in a 37°C incubator with 5% CO_2 until adherent cells reached about 90% confluence for downstream applications. BMMs adhered under the stimulation of M-CSF in complete α-MEM and no adherent cells were removed by washing.

Cell Viability Assay

To examine the effect of Pri on cell proliferation, BMMs (7×10^3 cells/well) were seeded in 96-well plates and allowed to adhere overnight. Next day, the medium was changed and supplemented with various concentrations of Pri for 48 or 96 h. Next, 10% CCK-8 solution was added to each well, and cells were incubated for 2 h at 37°C. The absorbance was subsequently measured at 450 nm using a microplate reader (Multiskan GO; Thermo Fisher Scientific, Waltham, MA).

Osteoclast Differentiation and TRAP Staining

To induce osteoclast differentiation, BMMs seeded in 96-well plates at a density of 7000 per well in complete α-MEM containing 25 ng/mL M-CSF and 100 ng/mL RANKL were treated without or with different concentrations of Pri (dose-dependent effect). For the time-dependent effects, BMMs were treated with 100 nM Pri, in the presence of 25 ng/mL M-CSF and 100 ng/mL RANKL, on Day 0 to Day 2 (D0–D2; early stage), Day 2 to Day 4 (D2–D4; mid-stage), Day 4 to Day 6 (D4–D6; late stage), and Day 0 to Day 6 (D0–D6). Medium was replaced every 2 days. The cells were fixed with 4% paraformaldehyde (PFA) for 30 min and stained for TRAP activity. TRAP-positive, multinucleated cells with three or more nuclei were quantified as osteoclasts and counted by Image-Pro Plus software (Media Cybernetics, Bethesda, MD).

F-actin Staining Assay

BMMs seeded in 96-well plates at a density of 7×10^3 cells/well were stimulated with 100 ng/mL RANKL without or with different concentrations of Pri until matured multinucleated osteoclasts formed. After 5 days of culture, cells were fixed in 4% PFA for 20 min, permeabilized with 0.5% Triton X-100 in PBS for 5 min, and further incubated with Actin-stain TM 488 Fluorescent Phalloidin to stain for actin cytoskeleton for 30 min at room

temperature. Nuclei were counterstained with DAPI for 5 min. Fluorescent images were captured under the Eclipse TS100 fluorescence microscope (Nikon, Japan).

Bone Resorption Assay

BMMs seeded onto bovine bone slices placed in a 96-well plate at a density of 1×10^4 cells/well were cultured in complete α-MEM containing 25 ng/mL M-CSF and 100 ng/mL RANKL for 4 days until osteoclasts began to form. The cells were further treated with different concentrations of Pri (0, 25, 50, or 100 nM) for 10 days. The slides were washed with 6% sodium hypochlorite solution to remove the cells and resorption pits were imaged using scanning electron microscopy (Thermo Fisher Scientific). The percentage of resorption area relative to total area under each treatment condition were measured using Image J software.

Real-Time Quantitative PCR

BMMs were seeded in a six-well plate at 2×10^5 cells per well and cultured with complete α-MEM medium containing 100 ng/mL RANKL and 25 ng/mL M-CSF. Additionally, BMMs were treated with or without 100 nM Pri for 1, 3, and 5 days or were treated with 0, 25, 50 or 100 nM Pri for 5 days until mature osteoclasts formed. TRIzol reagent (Thermo Fisher Scientific) was used to extract the total RNA from cultured cells according to the manufacturer's protocol. The concentration and purity of RNA were measured using NanoDrop2000 (Thermo Fisher Inc., Waltham, MA). Complementary DNA (cDNAs) samples were obtained by reverse transcription using Prime Script RT Master Mix. The resulting cDNAs were used as a template for qPCR using the SYBR Green-based Real-time PCR Master Mix (Takara Bio) as described in the manufacturer's protocol. The following cycling condition was used for all qPCR reactions: initial denaturation at 95 °C for 10 min; followed by 40 repeated cycles of 95 °C for 10 s, 60 °C for 20 s, and 72 °C for 20 s; and a final extension step at 72 °C for 90 s. The relative expressions of target genes were normalized to €-actin mRNA expression levels and calculated using $2-\Delta\Delta Ct$. The specific mouse primers that were used are listed in Table 1.

Protein Extraction and Western Blotting Analyses

Total proteins were extracted from BMMs that were pretreated with or without 100 nM Pri for 1 h and then stimulated with 100 ng/mL RANKL for 5, 15, 30, or 60 min for short-acting proteins. In addition, total proteins were extracted from BMMs treated with 100 ng/mL RANKL without or with 100 nM Pri for 1, 3, or 5 days for long-acting proteins. Cells were lysed in RIPA with protease and phosphatase inhibitors, and then mixed with loading buffer at 100°C for 5 min to obtain cytoplasm protein samples. M-CSF-dependent BMMs seeded in 10-cm plates at a density of 2×10^6 cells/well were pretreated with different concentrations of Pri (0, 25, 50, or 100 nM) for 60 min, followed by RANKL stimulated (100ng/mL) for 30 min. Cytoplasmic and nuclear protein fractions were prepared using the NE-PER Nuclear and Cytoplasmic Extraction Kit (Thermo Scientific, MA, USA) in accordance with the manufacturer's protocol. Protein lysates (30 μg) were separated by 10% SDS-PAGE gel and transferred onto PVDF membranes (Bio-Rad, Hercules, CA). The membranes were blocked with 5% non-fat milk for 2 h at room temperature and then incubated with specific primary antibodies overnight at 4°C. Furthermore, the membranes were washed three times in Tris-buffered saline with Tween (TBST) (5 min/time) and incubated with corresponding secondary antibodies for 1 h at room temperature. Western blot images were detected using a LAS-4000 Science Imaging System (Fujifilm, Tokyo, Japan).

Table 1 Mouse Primer Sets Used for qPCR

Genes	Primer Sequence, 5′–3′	
	Forward	**Reverse**
β-Actin	AGCCATGTACGTAGCCATCC	CTCTCAGCAGTGGTGGTGAA
TRAP	TCCTGGCTCAAAAAGCAGTT	ACATAGCCCACACCGTTCTC
CTSK	CTTCCAATACGTGCAGCAGA	TCTTCAGGGCTTTCTCGTTC
c-Fos	CCAGTCAAGAGCATCAGCAA	AAGTAGTGCAGCCCGGAGTA
NFATc1	CAGCTGCCGTCGCACTCTGGTC	CCCGGCTGCCTTCCGTCTCATA
V-ATPase d2	AAGCCTTTGTTTGACGCTGT	TTCGATGCCTCTGTGAGATG
DC-STAMP	CTTGCAACCTAAGGGCAAAG	TCAACAGCTCTGTCGTGACC

Ovariectomy (OVX) Mouse Model

The protocol for animal care and use of laboratory animals was conducted in accordance with National Institutes of Health Guide for Care and Use of Laboratory Animals (NIH Pub No 85-23, revised 1996), and approved by the Shaoxing People's Hospital Institutional Animal Care and Use Committee. Eighteen 2-month-old female C57BL/6 mice in SPF grade were randomly divided into three groups: Sham group, OVX group, and OVX + Pri group (10 mg/kg). We designed the dosages for in vivo intervention with Pri (10 mg/kg) according to the existing literatures.[18–21] The range of dosages in literatures was 1–50 mg/kg. We conducted a pre-experiment and found that 10 mg/kg is effective. The mice of OVX group and OVX + Pri group were anesthetized and underwent bilateral ovariectomy and those of Sham group underwent sham operation. All mice were intragastrically administered with Pri (10 mg/kg) or PBS (control) every 2 days for 2 months. Finally, all mice were sacrificed by cervical dislocation, and tibias and femurs were collected for mechanical testing, micro-CT scanning, and histological examination.

Micro-CT Scanning and Mechanical Testing

A materials-testing machine (4465; Instron, Norwood, MA, USA) was used to determine the mechanical properties of bilateral femora by destructive 3-point bend tests. The trabecular structure in the regions near the tibial growth plate was scanned at an isometric resolution of 18 mm and X-ray energy set to 80 kV and 100 mA. Three-dimensional structural parameters of tibia were analyzed, including bone volume/tissue volume (BV/TV), trabecular number (Tb.N), trabecular thickness, trabecular spacing (Tb.Sp), trabecular connectivity density (Conn.D), and structure model index (SMI).

Histological Analysis

Following microCT, tibias were decalcified with 10% EDTA for 3 weeks. After embedding in paraffin blocks, tibias were sliced into 5 mm thick sections for further TRAP activity analysis and hematoxylin-eosin staining. Sections were imaged under a high-quality microscope and analyzed using ImagePro Plus 6.0 software.

Statistical Analysis

The experiments were performed at least three times. The data in this study were analyzed by Student's *t*-test or one-way analysis of variance (ANOVA) and presented as mean ± standard deviation (SD) using GraphPad Prism version 8.0 software (GraphPad Software, San Diego, CA, USA). The results with p-values <0.05 were considered statistically significant.

Results

Pri Inhibits RANKL-Induced Osteoclastogenesis in vitro

Prior to the evaluation of the influence of Pri (Figure 1A) on osteoclastogenesis in vitro, we first assessed potential cytotoxic effects of various Pri concentrations on BMMs for 48 h and 96 h. As shown in Figure 1B, the viability of BMMs did not change after treatment with Pri at concentrations below 100 nM. Thus, for subsequent experiments, we chose Pri concentrations of 0, 25, 50, and 100 nM for the treatment of BMMs. To investigate the effect of Pri on RANKL-induced osteoclast differentiation, M-CSF-dependent BMMs were stimulated with 100 ng/mL RANKL in the presence of Pri at the indicated concentrations for 7 days. As shown in Figure 1C, numerous TRAP-positive multinucleate osteoclasts formed in the RANKL-treated group, whereas the number of osteoclasts in the Pri-treated group decreased in a dose-dependent manner. Furthermore, the size or cell spread area of osteoclasts in the Pri-treated group was similarly dose-dependently reduced, indicating a potential inhibitory effect on osteoclastogenesis. To evaluate the stage of osteoclastogenesis at which Pri exerted its inhibitory effect, RANKL-induced osteoclasts were treated with a Pri concentration of 100 nM at different time intervals during osteoclastogenesis. Pri only exerted a remarkable inhibitory effect on osteoclastogenesis on treatment Day 2 to 4 (Figure 1D).

Pri Inhibits F-Actin Ring and Bone Resorption in vitro

Given that Pri suppressed RANKL-induced osteoclastogenesis, its effect on osteoclast bone resorption was further detected in vitro. The F-actin ring is a critical structure of actively resorbing osteoclasts. The formation of mature F-actin ring was examined by immunofluorescence staining for actin and nuclei. Consistent with previous TRAP stained results, the size of actin ring structures and the number of nuclei per cell in Pri-treated group were

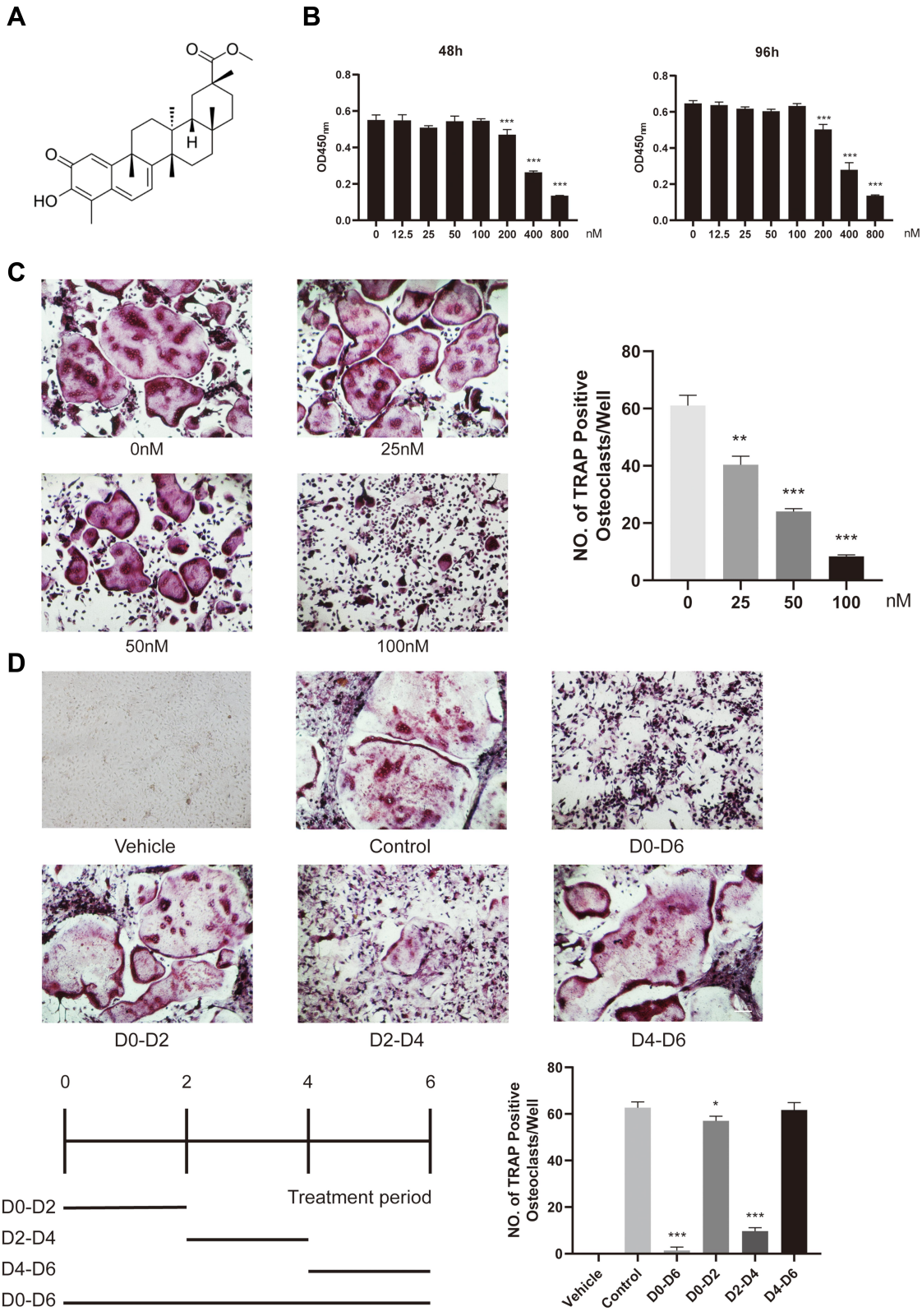

Figure 1 Pri attenuated RANKL-induced osteoclastogenesis in vitro. (**A**) The chemical structure of Pri. (**B**) M-CSF–dependent BMMs were treated with Pri for 48 and 96 h and analysed by CCK-8 (n=6). (**C**) Dose-dependent effect of Pri on osteoclastogenesis. Trap staining of osteoclasts treated with various concentrations of Pri (n=3). (**D**) Time-dependent effect of Pri on osteoclastogenesis. Trap staining of osteoclasts treated with 100nM Pri for indicated days (n=3). Data represent mean ± SD, *P < 0.05, **P < 0.01, ***P < 0.001 relative to RANKL-only-treated control.

strikingly reduced in a dose-dependent manner, especially at 100 nM (Figure 2A and C). Next, we evaluated whether the bone resorptive function of mature osteoclast was impaired after Pri treatment. Osteoclasts were cultured on bovine bone slices without or with indicated concentrations of Pri. As shown in Figure 2B and D, osteoclasts treated with Pri exhibited significantly reduced ability of bone resorption, especially at a concentration of 100 nM. These results indicate that Pri inhibits osteoclastic bone resorptive activity in vitro.

Pri Suppresses Osteoclast-Related Genes Expression in vitro

To deeply examine the underlying mechanism of the inhibitory effect of Pri, we measured the transcription levels of osteoclast-related genes such as DC-STAMP, CTSK, c-Fos, TRAP, V-ATPase d2, and NFATc1. The expression of these genes was markedly subdued by the adjunction of Pri, compared with the control (Figure 3A). Without treatment with Pri, the mRNA expression levels of osteoclast marker genes, including TRAP, CTSK, c-Fos, NFATc1, DC-STAMP, and V-ATPase d2, were all strikingly upregulated on induction by RANKL during the osteoclast differentiation process. On the contrary, the concomitant application of Pri and RANKL significantly downregulated these six genes (Figure 3A). Consistent with the antiresorptive effect of Pri on mature osteoclasts, our qRT-PCR analysis confirmed that Pri inhibited these genes' expression in a dose-dependent manner (Figure 3B). These results confirm the function of Pri in inhibiting RANKL-induced osteoclast marker genes' expression in vitro.

Pri Attenuates RANKL-Induced Osteoclastogenesis by Inhibiting MAPK and PI3K-AKT Signaling Pathways

Of the signaling pathways activated, NF-κB and MAPK are important in the early phase of osteoclast differentiation process.[22] RANKL stimulation clearly promoted phosphorylation of P65, and all three members of the MAPK cascade, ERK, p38, and JNK, especially at 5 and 15 minutes. As shown in Figure 4A and B, Pri treatment did not affect IκBα and P65 of the NF-κB signaling pathway. Moreover, after RANKL stimulation, the expression of p65 in the nucleus was increased and the IκBα expression in the cytoplasm was decreased. Nevertheless, Pri did not affect the translocation of the p65 and IκBα degradation induced by RANKL (Figure 4C and D). On the contrary, there is no significant inhibitory effect of Pri on phosphorylation of P38 of the MAPK signaling pathway, while the phosphorylation of ERK and JNK was significantly attenuated by Pri (Figure 4A and B). In addition to the MAPK/NF-κB pathway, the AKT-NFATc1 signalling axis has also been reported to be significant in osteoclast formation.[23] Pri treatment significantly attenuated the phosphorylation of AKT compared with the control but did not affect the expression level of PI3K (Figure 4A and B). The results showed that Pri can suppress the RANKL-induced activation of the MAPK and PI3K-AKT signaling pathways.

Pri Inhibits RANKL-Induced c-Fos/c-Jun and NFATc1 Signaling Pathway

Further exploration of the effect of Pri on downstream transcriptional factors was focused on three transcriptional factors critical for osteoclastogenesis—c-Fos, c-Jun, and NFATc1. As shown in Figure 5A and B, RANKL robustly induced the expression of c-Fos and c-jun protein over a 5-day culture period. Treatment with Pri, however, downregulated c-Fos and c-jun expression on Day 3 and 5 of RANKL stimulation. Similarly, we found that protein expression levels of NFATc1 increased in a time-dependent manner at Day 0, 1, 3, and 5 in the presence of RANKL (Figure 5A and B). However, Pri treatment significantly inhibited the protein expression levels of NFATc1 at Day 3 and 5. Moreover, Pri treatment attenuated these protein expressions in a dose-dependent manner (Figure 5C and D). Overall, these results suggest that Pri inhibits osteoclastogenesis through the early MAPK and PI3K-AKT signaling pathways, which are necessary for c-Fos/c-Jun and NFATc1 induction.

Pri Protects Against OVX-Induced Bone Loss and Reduction of Mechanical Strength

To examine the in vivo efficacy of Pri against osteoclast activity, we next established an OVX model. We observed decreased bone stiffness in the OVX groups based on results obtained from a materials-testing machine, compared with the sham-treated group. However, Pri was shown to attenuate this OVX-induced deterioration in the mechanical properties of the bone (Figure 6A). This was further confirmed by micro-CT analysis. Micro-CT 3D image showed that Pri significantly protected OVX-induced trabecular bone loss

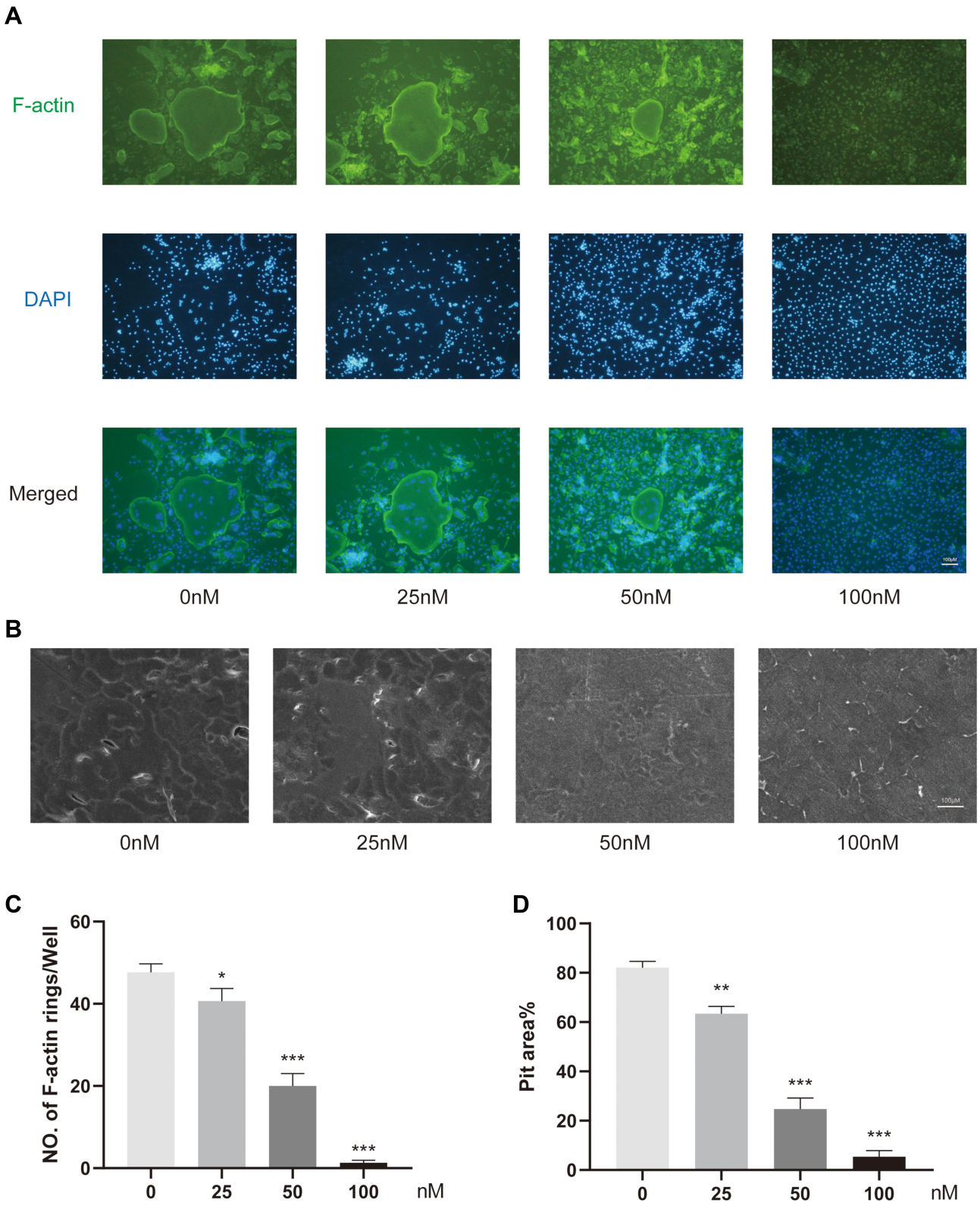

Figure 2 Pri inhibited F-actin ring and bone resorption in vitro. (**A**) The F-actin ring of osteoclasts were stained by Actin-stain TM 488 Fluorescent Phalloidin and nuclei stained by DAPI. (**B**) Representative SEM images of bone resorption lacunae. (**C**) The number of F-actin rings was quantified (n=3). (**D**) The percentage of bone resorption lacunae area was quantified (n=3). Data represent mean ± SD, *P < 0.05, **P < 0.01, ***P < 0.001 relative to RANKL-only-treated control.

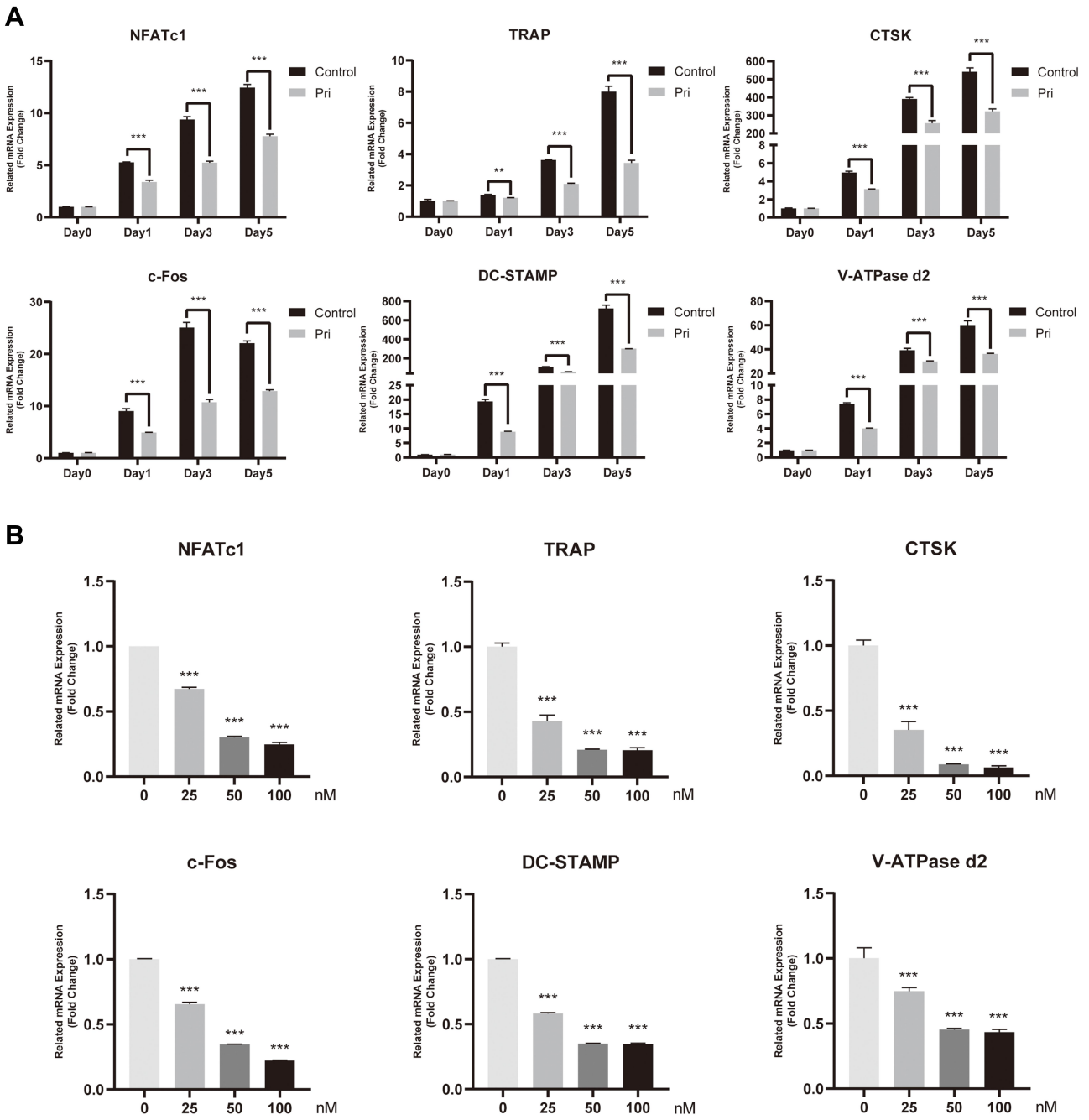

Figure 3 Pri suppressed RANKL-induced expression of osteoclastogenesis-related genes. (**A**) Time-dependent mRNA expression profile of osteoclast-specific genes (n=3). (**B**) Dose-dependent mRNA expression profile of osteoclast-specific genes (n=3). Data represent mean ± SD, **P < 0.01, ***P < 0.001 relative to RANKL-only-treated control.

(Figure 6B). The parameters of bone volume/tissue volume (BV/TV), trabecular thickness (Tb.Th), trabecular number (Tb.N), trabecular separation (Tb.Sp), Conn.D (trabecular connectivity density), and SMI (structure model index) were measured, and we observed an increase in BV/TV and Tb.N and a decrease in Tb. Sp and Conn.D in the OVX + Pri group compared to those in the OVX group (Figure 6C).

Histological assessment further confirmed that Pri prevented OVX-induced bone loss (Figure 7A). The histological analysis demonstrated that Pri treatment increased BV/TV compared with the OVX group (Figure 7B). Moreover, an increased number of mature osteoclasts (TRAP-positive cells) were observed in the OVX group, whereas Pri treatment showed a decreased number of

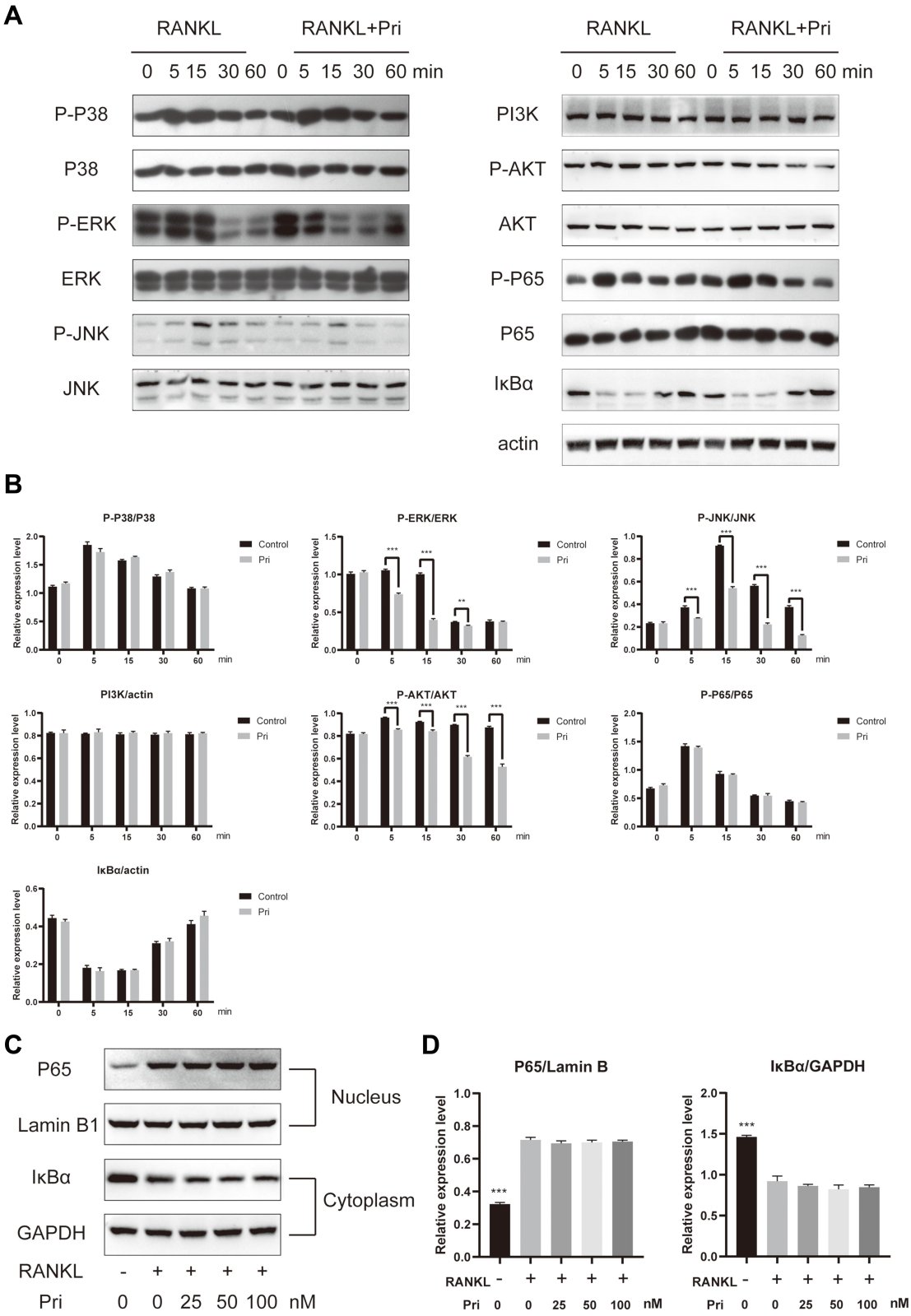

Figure 4 Pri attenuated RANKL-stimulated ERK, JNK and AKT signaling pathways. (**A**) Pri inhibited the phosphorylation of ERK, JNK and AKT. (**B**) Quantification of MAPK, NF-κB and AKT signaling pathway proteins expression levels (n=3). (**C**) Pri did not affect the translocation of the p65 and IκBα degradation induced by RANKL. (**D**) Quantification of nuclear p65 and cytosolic IκBα expression levels (n=3). Data represent mean ± SD, **P < 0.01, ***P < 0.001 relative to RANKL-only-treated control.

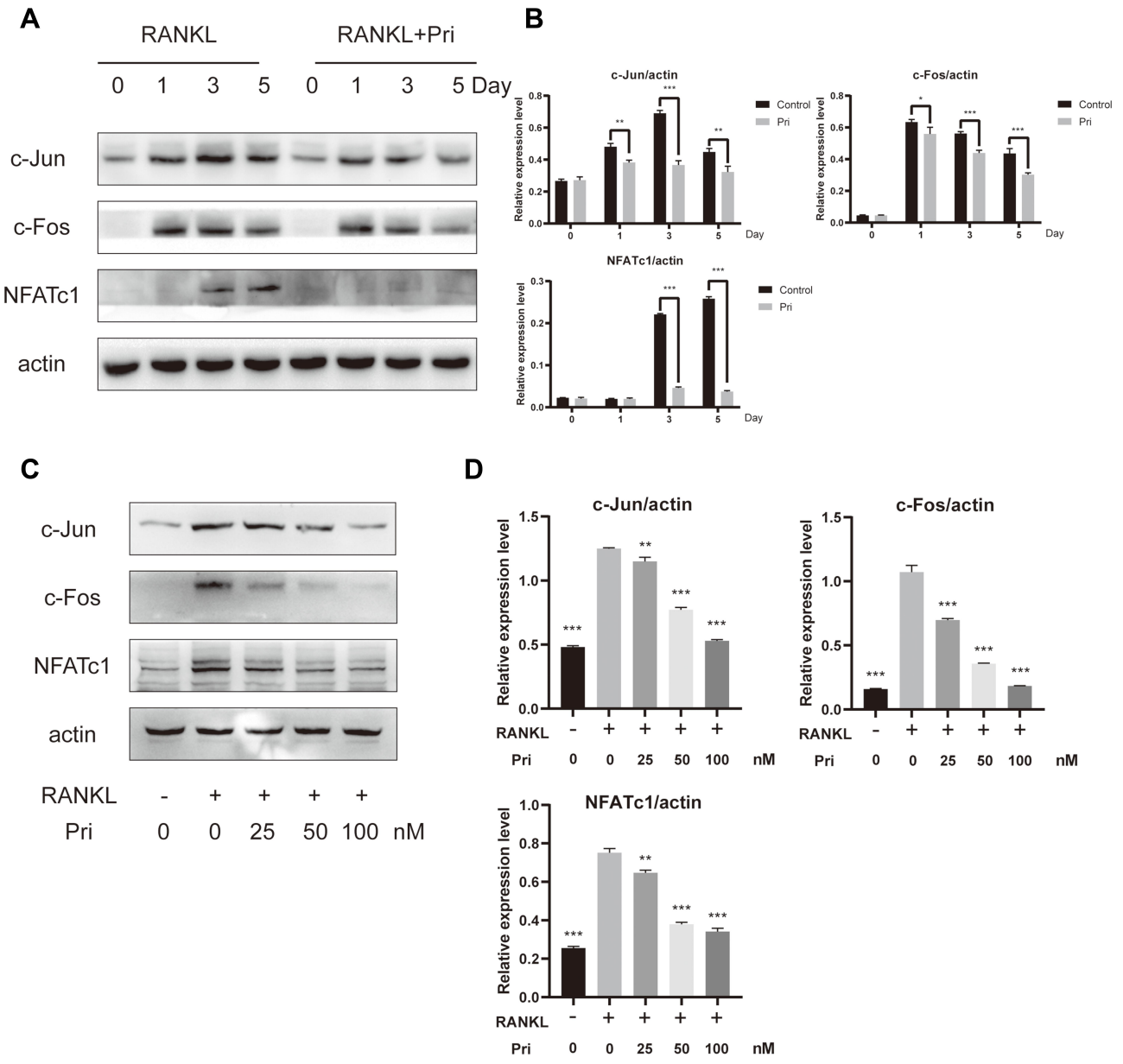

Figure 5 Pri inhibits RANKL-induced c-Fos/c-Jun and NFATc1 signaling pathway. (**A** and **C**) Pri suppressed RANKL-induced c-Jun, c-Fos and NFATc1 protein expression. (**B** and **D**) Quantification of c-Jun, c-Fos and NFATc1 expression levels (n=3). Data represent mean ± SD, *P < 0.05, **P < 0.01, ***P < 0.001 relative to RANKL-only-treated control.

mature osteoclasts (Figure 7B). Collectively, our data demonstrate that Pri has potential as therapeutic agent against osteolytic diseases such as postmenopausal osteoporosis.

Discussion

Postmenopausal osteoporosis and other osteolytic bone diseases are often caused by elevated osteoclast formation and/or increased osteoclastic bone resorption.[24] Therefore, osteoclasts have long been the primary cellular targets for the identification and development of therapeutic agents for the effective treatment of osteoporosis. In our study, we demonstrated that Pri significantly inhibits osteoclastogenesis and bone resorption by downregulating osteoclast-related gene expression and suppressing RANKL-induced activation of ERK, JNK MAPK, and PI3K-AKT signaling pathways in vitro. In addition, Pri was found to prevent OVX-induced bone loss in vivo by micro-CT and histological analysis.

Our present study demonstrated that Pri could markedly suppress osteoclastogenesis at doses of 50 and 100 nM without cytotoxicity on BMMs. Intriguingly, a significant

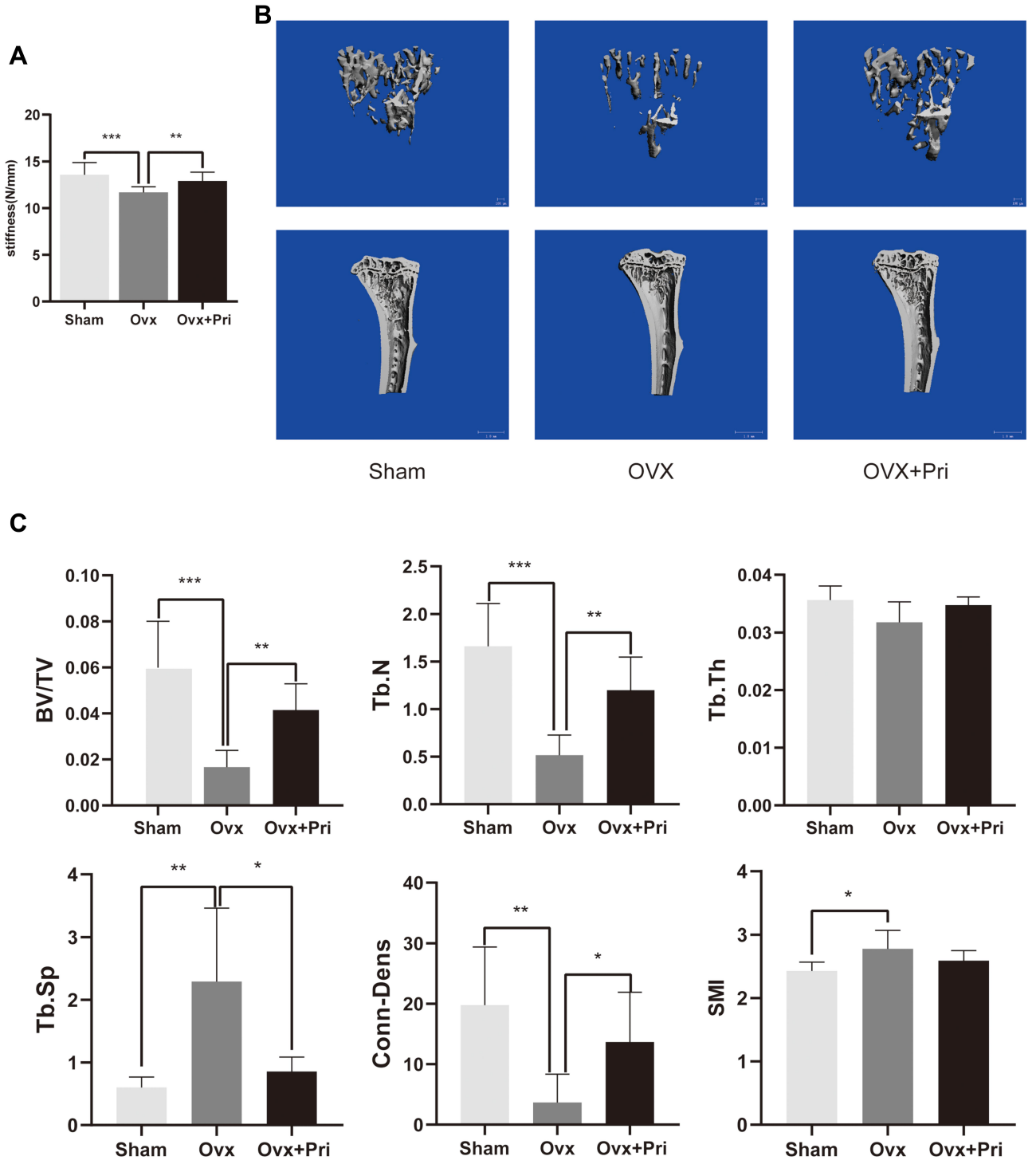

Figure 6 Pri reduced OVX-induced bone loss in vivo. (**A**) Mechanical properties of femurs were measured (n=6). (**B**) Representative 3D micro-CT images of mice in Sham, OVX, and OVX + Pri groups. (**C**) Quantitative analysis of morphometric parameters of BV/TV, Tb.N, Tb.Th, Tb.Sp, Conn.D, and SMI (n = 6). Data represent mean ± SD, *P < 0.05, **P < 0.01, ***P < 0.001 relative to their respective controls.

inhibitory effect on osteoclast formation was observed with Pri treatment at a mid-stage of osteoclastogenesis. Consistent with previous TRAP stained results, Pri did not affect IκBα and P65 of the NF-κB signaling pathway (at an early stage), but inhibited c-Fos/c-Jun and NFATc1 (at a late stage) of osteoclastogenesis, subsequently attenuating the expression of osteoclast-related as shown by real-time PCR and Western blot results. Pri also inhibited osteoclast

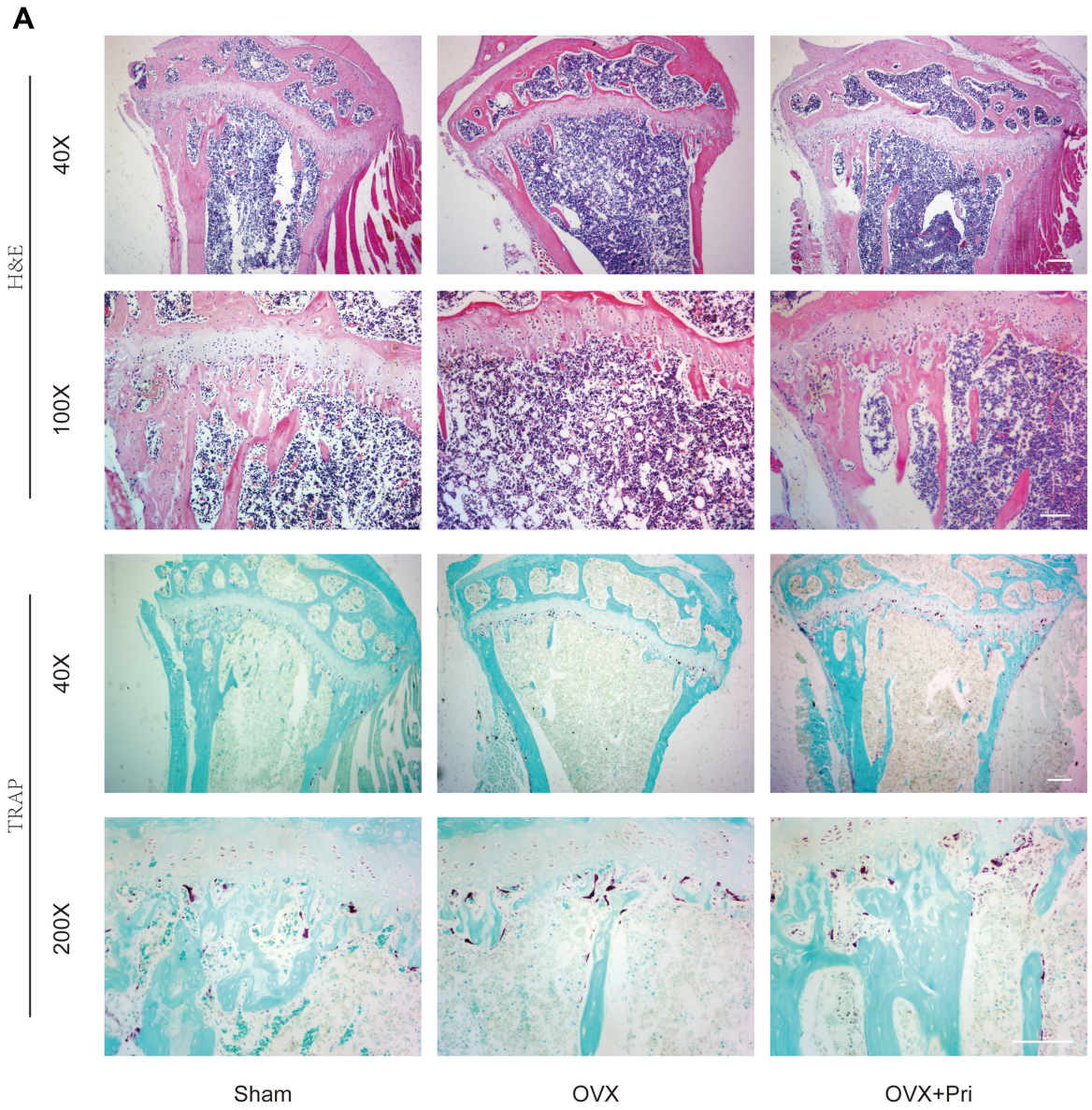

Figure 7 Histologic and histomorphometric evaluation of Pri treatment in OVX-induced bone loss. (**A**) Decalcified tibias from mice in Sham, OVX, and OVX +Pri groups were stained by H&E and TRAP. (**B**) Quantitative analyses of BV/TV, number of TRAP-positive osteoclasts and percentage of osteoclast surface to bone surface (Oc.S/BS,%) (n = 6). Data represent mean ± SD, **P < 0.01, ***P < 0.001 relative to their respective controls.

function including F-actin ring formation and bone resorption. Animal experiment results showed that Pri protected osteoporosis after OVX operation in vivo. Our study indicated that Pri can be used as a treatment for patients with osteoporosis.

Binding of RANKL to receptor RANK results in the activation of several key intracellular signaling pathways, some of which are the NF-κB and MAPKs pathways during the very early phase of osteoclastogenesis.[25] RANKL stimulates MAPK signaling, which consists of three family members, ERK, p38, and JNK, to activate AP-1 (c-Fos and c-Jun) to promote osteoclast formation.[26–28] P38 signaling is predominantly involved in osteoclast differentiation rather than osteoclast function.[29] JNK and ERK are also necessary for efficient osteoclast formation, whilst ERK is required for maintenance of cell polarity during bone resorption.[30,31] Our data showed that Pri inhibited the phosphorylation of ERK and JNK but had no effect on p38 activation.

Under steady-state conditions, inactive p65/p50 NF-κB proteins are bound to inhibitory κB proteins (IκBs) and sequestered in the cytoplasm of the cell. After stimulation with RANKL, the two catalytic components of I-kappaB kinase (IKK), IKKα and IKKβ, are activated, leading to the rapid phosphorylation and proteasomal degradation of IκBs. This enables phosphorylated p65 to translocate into the nucleus and bind to specific DNA sites to drive transcription and expression of osteoclastogenesis-related genes.[32,33] Despite its importance in osteoclast formation, Pri treatment did not inhibit RANKL-induced IκBα degradation or p65 phosphorylation, suggesting that the anti-osteoclastic effect is not the result of NF-κB inactivation.

Activation of the AKT pathway, a downstream mediator of RANK signaling, plays an important role in regulating cell proliferation, differentiation, and apoptosis, and it has been reported that inhibition of AKT activation could prevent RANKL-induced osteoclastogenesis.[34,35] In this study, we found that Pri dramatically suppressed the phosphorylation of AKT activated by RANKL in BMMs. Activation of ERK and p38 signaling is important for the downstream induction and upregulation of transcription factors c-Fos, an essential component of the AP-1 transcription factor complex.[36] More importantly, c-Fos is located in upstream of NFATc1, which could directly regulate the expression of NFATc1.[37] In addition, NFATc1 has been shown to be a key transcription factor that plays an important role in osteoclastogenesis.[38] NFATc1 can regulate varying osteoclast-specific genes involved in osteoclast differentiation and function, including c-Fos, TRAP, CTSK, V-ATPase d2, and DC-STAMP.[39] DC-STAMP is an essential molecule for mononuclear osteoclast fusion and giant cell formation that increases the absorbing activity of osteoclasts.[40,41] Our biochemical analyses demonstrated that Pri significantly reduced expression of NFATc1 both at protein and mRNA levels. Equally, Pri downregulated the levels of c-Fos, TRAP, CTSK, V-ATPase d2, and DC-STAMP, indicating that Pri can inhibit RANKL-induced osteoclasts activity. Collectively, we provided significant cellular and biochemical evidence for the antiosteoclastogenic effects of Pri, which are mediated by the inhibition of ERK/JNK/AKT/c-Fos/NFATc1 signaling pathways.

Considering the promising effect of Pri in vitro, we further evaluated the therapeutic potential of Pri in the prevention of osteoclast-mediated bone loss in vivo using an OVX-induced osteoporosis mouse model. OVX mouse is an established animal model for the investigation of estrogen deficiency-induced bone loss and the treatment effects of postmenopausal osteoporosis.[42] Micro CT and morphometric analysis showed that Pri treatment significantly reduced bone loss in OVX-induced mice by improving bone volume and trabecular bone parameters. Histological assessments showed that Pri treatment reduced the number of TRAP-positive osteoclasts and the area of osteoclast activity per bone surface.

Despite the novel findings of our study, we cannot exclude the possibility that Pri might affect osteoblastic bone formation. In addition, we cannot rule out the possibility that the anti-inflammatory property of Pri contributed towards the biological effects of Pri on OVX-induced bone loss. Thus, further investigations are needed.

In summary, we demonstrated that Pri significantly inhibited osteoclastogenesis and bone resorption in vitro and protected OVX-induced bone loss in vivo. These findings suggest that Pri might be a potential agent for the treatment of osteoclast-related diseases like osteoporosis.

Abbreviations

Pri, pristimerin; BMMs, bone marrow-derived macrophages; NFATc1, nuclear factor of activated T-cell cytoplasmic 1; M-CSF, macrophage colony-stimulating factor; RANKL, receptor activation of NF-κB ligand; TRAP, tartrate-resistant acid phosphatase; OVX, ovariectomy.

Acknowledgments

This study was funded by the National Natural Science Foundation of China (grant no. 81572126 and 81871801), the Natural Science Foundation of Zhejiang Province (grant no. LY15H060005), and the Zhejiang Basic Public Welfare Research Project (LGF20H060011 and LGF18H060010).

Disclosure

The paper has been polished by a professional English native speaker.

The authors declare no other potential conflicts of interest for this work.

References

1. Chen X, Wang Z, Duan N, Zhu G, Schwarz EM, Xie C. Osteoblast-osteoclast interactions. *Connect Tissue Res*. 2018;59(2):99–107. doi:10.1080/03008207.2017.1290085
2. Lorenzo J. The many ways of osteoclast activation. *J Clin Invest*. 2017;127(7):2530–2532. doi:10.1172/JCI94606
3. Pereira M, Petretto E, Gordon S, Bassett JHD, Williams GR, Behmoaras J. Common signalling pathways in macrophage and osteoclast multinucleation. *J Cell Sci*. 2018;131:11. doi:10.1242/jcs.216267
4. Ensrud KE, Crandall CJ. Osteoporosis. *Ann Intern Med*. 2017;167(3): Itc17itc32. doi:10.7326/AITC201708010
5. Meunier PJ, Roux C, Ortolani S, et al. Effects of long-term strontium ranelate treatment on vertebral fracture risk in postmenopausal women with osteoporosis. *Osteoporosis International*. 2009;20 (10):1663–1673. doi:10.1007/s00198-008-0825-6
6. Compston JE, McClung MR, Leslie WD. Osteoporosis. *Lancet*. 2019;393(10169):364–376. doi:10.1016/S0140-6736(18)32112-3
7. Kennel KA, Drake MT. Adverse effects of bisphosphonates: implications for osteoporosis management. *Mayo Clin Proc*. 2009;84(7):-632–637; quiz 638. doi:10.1016/S0025-6196(11)60752-0
8. Ikebuchi Y, Aoki S, Honma M, et al. Coupling of bone resorption and formation by RANKL reverse signalling. *Nature*. 2018;561 (7722):195–200. doi:10.1038/s41586-018-0482-7
9. Cao X. RANKL-RANK signaling regulates osteoblast differentiation and bone formation. *Bone Research*. 2018;6(35).
10. A-F N, et al. The role of osteoclast-associated receptor in osteoimmunology. *J Immunol*. 2011;186(1):13–18.
11. Sobacchi C, Schulz A, Coxon F, Villa A, Helfrich M. Osteopetrosis: genetics, treatment and new insights into osteoclast function. *Nat Rev Endocrinol*. 2013;9(9):522–536. doi:10.1038/nrendo.2013.137
12. Lu Z, Jin Y, Chen C, Li J, Cao Q, Pan J. Pristimerin induces apoptosis in imatinib-resistant chronic myelogenous leukemia cells harboring T315I mutation by blocking NF-kappaB signaling and depleting Bcr-Abl. *Mol Cancer*. 2010;9:112. doi:10.1186/1476-4598-9-112
13. JY B, MJ K, DY E, et al. Reactive oxygen species-dependent activation of Bax and poly (ADP-ribose) polymerase-1 is required for mitochondrial cell death induced by triterpenoid pristimerin in human cervical cancer cells. *Mol Pharmacol*. 2009;76(4):734–744. doi:10.1124/mol.109.056259
14. H Y KRL-P, et al. Pristimerin induces apoptosis by targeting the proteasome in prostate cancer cells. *J Cell Biochem*. 2008;103 (1):234–244. doi:10.1002/jcb.21399
15. Liang J, Yuan S, Wang X, et al. Attenuation of pristimerin on TNF-α-induced endothelial inflammation. *Int Immunopharmacol*. 2020;82:106326. doi:10.1016/j.intimp.2020.106326
16. LN W, et al. Pristimerin enhances recombinant adeno-associated virus vector-mediated transgene expression in human cell lines in vitro and murine hepatocytes in vivo. *J Integr Med*. 2014;12 (1):20–34. doi:10.1016/S2095-4964(14)60003-0
17. E-A DS, E-H KM, et al. Pristimerin protects against doxorubicin-induced cardiotoxicity and fibrosis through modulation of Nrf2 and MAPK/NF-kB signaling pathways. *Cancer Manag Res*. 2019;11:47–61.
18. Sun J, Xu H, Zhao L, et al. Induction of cell-cycle arrest and apoptosis in human cholangiocarcinoma cells by pristimerin. *J Cell Biochem*. 2019.
19. Shaaban A, El-Kashef D, Hamed M, El-Agamy D. Protective effect of pristimerin against LPS-induced acute lung injury in mice. *Int Immunopharmacol*. 2018;59:31–39. doi:10.1016/j.intimp.2018.03.033
20. Cevatemre B, Erkısa M, Aztopal N, et al. A promising natural product, pristimerin, results in cytotoxicity against breast cancer stem cells in vitro and xenografts in vivo through apoptosis and an incomplete autophagy in breast cancer. *Pharmacol Res*. 2018;129:500–514. doi:10.1016/j.phrs.2017.11.027
21. Zhao H, Wang C, Lu B, et al. Pristimerin triggers AIF-dependent programmed necrosis in glioma cells via activation of JNK. *Cancer Lett*. 2016;374(1):136–148. doi:10.1016/j.canlet.2016.01.055
22. Takayanagi H. Mechanistic insight into osteoclast differentiation in osteoimmunology. *J Molecular Med*. 2005;83(3):170–179. doi:10.1007/s00109-004-0612-6
23. Lu X, He W, Yang W, et al. Dual effects of baicalin on osteoclast differentiation and bone resorption. *J Cell Mol Med*. 2018;22 (10):5029–5039. doi:10.1111/jcmm.13785
24. Tian K, Su Y, Ding J, et al. Hederagenin protects mice against ovariectomy-induced bone loss by inhibiting RANKL-induced osteoclastogenesis and bone resorption. *Life Sci*. 2020;244:117336. doi:10.1016/j.lfs.2020.117336
25. JH K. Signaling Pathways in Osteoclast Differentiation. *Chonnam Med J*. 2016;52(1):12–17. doi:10.4068/cmj.2016.52.1.12
26. Matsuo K, Owens J, Tonko M, Elliott C, Chambers T, Wagner E. Fosl1 is a transcriptional target of c-Fos during osteoclast differentiation. *Nat Genet*. 2000;24(2):184–187. doi:10.1038/72855
27. EF W. Fos/AP-1 proteins in bone and the immune system. *Immunol Rev*. 2005;208:126–140. doi:10.1111/j.0105-2896.2005.00332.x
28. JM K, YS L, YS K, et al. Homocysteine enhances bone resorption by stimulation of osteoclast formation and activity through increased intracellular ROS generation. *J Bone Mineral Res*. 2006;21 (7):1003–1011.
29. Pengjam Y, Madhyastha H, Madhyastha R, Yamaguchi Y, Nakajima Y, Maruyama M. Anthraquinone glycoside aloin induces osteogenic initiation of MC3T3-E1 cells: involvement of MAPK mediated Wnt and Bmp signaling. *Biomol Ther (Seoul)*. 2016;24 (2):123–131. doi:10.4062/biomolther.2015.106
30. Li X, Udagawa N, Itoh K, et al. p38 MAPK-mediated signals are required for inducing osteoclast differentiation but not for osteoclast function. *Endocrinology*. 2002;143(8):3105–3113. doi:10.1210/endo.143.8.8954
31. He Y, Staser K, Rhodes SD, et al. Erk1 positively regulates osteoclast differentiation and bone resorptive activity. *PLoS One*. 2011;6(9): e24780. doi:10.1371/journal.pone.0024780
32. Zhang Q, Lenardo M, Baltimore D. 30 Years of NF-κB: A blossoming of relevance to human pathobiology. *Cell*. 2017;168:37–57. doi:10.1016/j.cell.2016.12.012
33. A-A Y. NF-κB signaling and bone resorption. *Osteoporosis International*. 2013;24(9):2377–2386. doi:10.1007/s00198-013-2313-x
34. Matsumoto T, Nagase Y, Iwasawa M, et al. Distinguishing the proapoptotic and antiresorptive functions of risedronate in murine osteoclasts: role of the Akt pathway and the ERK/Bim axis. *Arthritis Rheum*. 2011;63(12):3908–3917. doi:10.1002/art.30646

35. Gingery A, Bradley E, Shaw A, Oursler M. Phosphatidylinositol 3-kinase coordinately activates the MEK/ERK and AKT/NFkappaB pathways to maintain osteoclast survival. *J Cell Biochem*. 2003;89(1):165–179. doi:10.1002/jcb.10503
36. AJ W, RJ D. Transcription factor AP-1 regulation by mitogen-activated protein kinase signal transduction pathways. *J Molecular Med*. 1996;74(10):589–607. doi:10.1007/s001090050063
37. BC J, JH K. ATF3 modulates calcium signaling in osteoclast differentiation and activity by associating with c-Fos and NFATc1 proteins. *Bone*. 2017;95:33–40. doi:10.1016/j.bone.2016.11.005
38. Yamashita T, Yao Z, Li F, et al. NF-kappaB p50 and p52 regulate receptor activator of NF-kappaB ligand (RANKL) and tumor necrosis factor-induced osteoclast precursor differentiation by activating c-Fos and NFATc1. *J Biol Chem*. 2007;282(25):18245–18253. doi:10.1074/jbc.M610701200
39. Song I, Kim J, Kim K, Jin H, Youn B, Kim N. Regulatory mechanism of NFATc1 in RANKL-induced osteoclast activation. *FEBS Lett*. 2009;583(14):2435–2440. doi:10.1016/j.febslet.2009.06.047
40. Zhang C, Dou C, Xu J, Dong S. DC-STAMP, the key fusion-mediating molecule in osteoclastogenesis. *J Cell Physiol*. 2014;229(10):1330–1335. doi:10.1002/jcp.24553
41. Yagi M, Miyamoto T, Sawatani Y, et al. DC-STAMP is essential for cell-cell fusion in osteoclasts and foreign body giant cells. *J Exp Med*. 2005;202(3):345–351. doi:10.1084/jem.20050645
42. Qi M, Zhang L, Ma Y, et al. Autophagy maintains the function of bone marrow mesenchymal stem cells to prevent estrogen deficiency-induced osteoporosis. *Theranostics*. 2017;7(18):4498–4516. doi:10.7150/thno.17949

Drug Design, Development and Therapy Dovepress

Publish your work in this journal

Drug Design, Development and Therapy is an international, peer-reviewed open-access journal that spans the spectrum of drug design and development through to clinical applications. Clinical outcomes, patient safety, and programs for the development and effective, safe, and sustained use of medicines are a feature of the journal, which has also been accepted for indexing on PubMed Central. The manuscript management system is completely online and includes a very quick and fair peer-review system, which is all easy to use. Visit http://www.dovepress.com/testimonials.php to read real quotes from published authors.

Submit your manuscript here: https://www.dovepress.com/drug-design-development-and-therapy-journal